

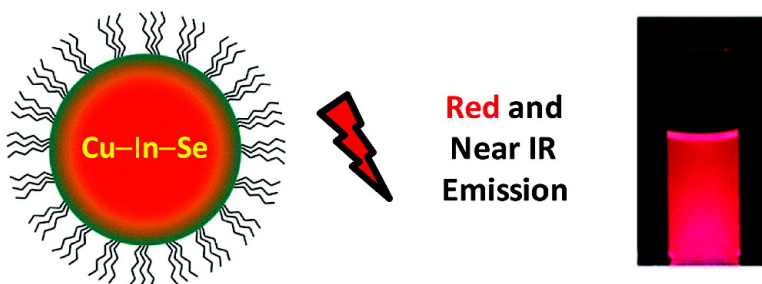
Communication

Ternary I#III#VI Quantum Dots Luminescent in the Red to Near-Infrared

Peter M. Allen, and Mounji G. Bawendi

J. Am. Chem. Soc., **2008**, 130 (29), 9240-9241 • DOI: 10.1021/ja8036349 • Publication Date (Web): 27 June 2008

Downloaded from <http://pubs.acs.org> on February 8, 2009



More About This Article

Additional resources and features associated with this article are available within the HTML version:

- Supporting Information
- Access to high resolution figures
- Links to articles and content related to this article
- Copyright permission to reproduce figures and/or text from this article

[View the Full Text HTML](#)

Ternary I–III–VI Quantum Dots Luminescent in the Red to Near-Infrared

Peter M. Allen and Mounji G. Bawendi*

Department of Chemistry, Massachusetts Institute of Technology, 77 Massachusetts Avenue, Cambridge, Massachusetts 02139

Received May 15, 2008; E-mail: mgb@mit.edu

We report the synthesis of a size series of copper indium selenide (Cu–In–Se) quantum dots (QDs) of various stoichiometries exhibiting photoluminescence (PL) from the red to the near-infrared (NIR). The synthetic method is modular, and we have extended it to the synthesis of luminescent AgInSe₂ QDs. Previous reports on QDs luminescent in the NIR region have been primarily restricted to binary semiconductor systems, such as InAs, PbS, and CdTe.^{1–3} This work seeks to expand the availability of luminescent QD materials to ternary I–III–VI semiconductor systems. Ternary I–III–VI QDs with tunable band gaps (E_g) in the NIR region are of interest for applications in photovoltaic cells and as biological imaging agents.^{4,5}

In bulk Cu–In–Se semiconductors, band edge PL is rarely observed at room temperature due to fast nonradiative relaxation promoted by defect sites.⁶ Previous work on Cu–In–Se QDs has not reported PL.^{7–9} Reports on I–III–VI sulfide QD systems have incorporated zinc in order to enhance quantum yields (QYs) and tune emission properties.^{10,11} Here, we present a ternary semiconductor system where PL is tuned by QD size.

Previous Cu–In–Se QD synthetic work has included the use of single source precursors.⁸ However, the synthetic methodology using single source precursors was not amenable to the facile introduction of capping ligands, preventing adequate size control and surface passivation. Other reports have utilized CuCl, InCl₃, and tri-*n*-octylphosphine selenide (TOPSe) to synthesize Cu–In–Se QDs but did not produce QDs with distinct absorption features.^{7,9} Mechanistic studies on the role of TOPSe in a “hot injection” QD synthesis have demonstrated two potential reaction pathways for the formation of QDs: (i) the generation of M⁰ before reaction with TOPSe and (ii) the direct reaction of carboxylic/phosphonic acid ligands with TOPSe.^{12,13} In the absence of these pathways, TOPSe may not be an adequate precursor in combination with CuCl and InCl₃ for a hot injection Cu–In–Se QD synthesis.

In our synthetic approach, we have selected bis(trimethylsilyl)selenide [(Me₃Si)₂Se] as the chalcogenide precursor. The choice of copper precursors was limited by the tendency of Cu(I) to disproportionate in solution.¹⁴ Previous reports have demonstrated that copper and indium halides are stable sources of Cu(I) and In(III).^{7,9} A combination of metal halides and a chalcogenide silane precursor was selected in order to exploit a metathetical dehalosilylation reaction scheme, eliminating the need to generate elemental copper and indium in solution.¹⁵

A combination of tri-*n*-octylphosphine (TOP) and oleylamine (OA) was used as a coordinating solvent. The metal halides can be readily dispersed in TOP or OA to form homogeneous solutions. In a typical synthesis, a solution of metal halides in TOP and OA was heated to 280–360 °C followed by the swift injection of a solution of (Me₃Si)₂Se in TOP and subsequent growth at temperatures ranging from 200 to 280 °C. The size and composition of the prepared QDs can be tuned by the choice of metal halides and growth temperatures.

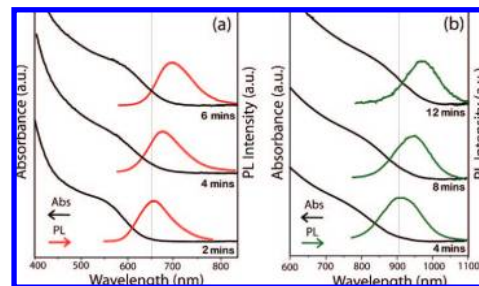


Figure 1. Absorbance and PL of (a) CuIn₅Se₈ QDs grown from 650 to 700 nm with injection at 280 °C and growth at 210 °C from CuI and InI₃ precursors and (b) CuIn_{2.3}Se₄ QDs grown from 900 to 975 nm with identical conditions as in (a) but with CuCl and InCl₃ precursors.

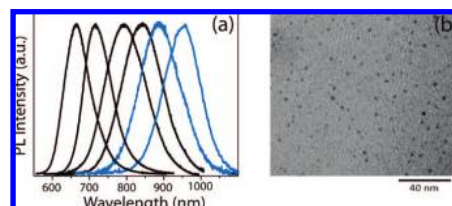


Figure 2. (a) PL spanning from the red to the NIR (650–975 nm) from CuIn₅Se₈ QDs ranging from ~2.0 to 3.5 nm mean diameter (black) and from CuIn_{2.3}Se₄ QDs (~3.0–3.5 nm mean diameter) (blue). (b) TEM of 3.0 ± 0.5 nm CuIn_{2.3}Se₄ QDs.

The CuI and InI₃ precursors produced QDs of composition CuIn₅Se₈, with PL in the red and NIR (Figure 1a). The elemental compositions of the QDs resulting from the reaction of the iodide precursors with (Me₃Si)₂Se were found to be largely independent of reaction conditions (Figure S1). In the case of the CuCl and InCl₃ precursors, it was possible to tune the composition of the prepared QDs from CuIn_{1.5}Se₃ to CuIn_{2.3}Se₄ (Figure 1b) by varying the reaction temperature (Table S1). This synthetic method produced a size series of Cu–In–Se QDs of various stoichiometries luminescent from the red to NIR (Figure 2a). The generality of this synthetic approach was demonstrated by replacing the metal halide precursors with AgI and InI₃, which successfully synthesized AgInSe₂ QDs with luminescence from orange to red (Figure S2).

Transmission electron microscopy (TEM) indicates the QDs are spherical in nature with an approximately 15% rms deviation in size from the mean QD diameter (Figure 2b and Figure S3). The sizes determined by TEM measurements are in agreement with those obtained by Scherrer analysis, suggesting the crystalline coherence length extends over the entire QD.

Bulk Cu–In–Se exists primarily in either a tetragonal chalcopyrite or a high temperature cubic sphalerite phase.¹⁶ The observed wide-angle X-ray scattering (WAXS) and elemental compositions of the Cu–In–Se QDs were found to be well-described by an ordered vacancy chalcopyrite structure. Analysis

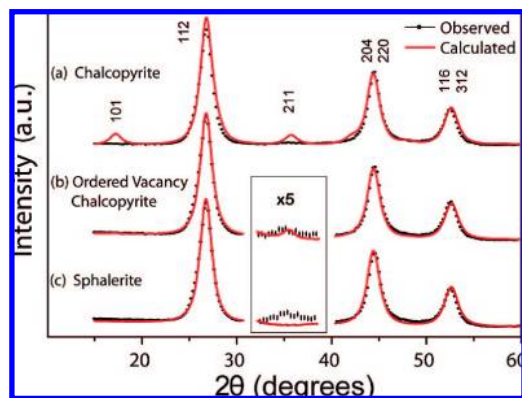


Figure 3. Comparison of experimental WAXS to calculated patterns for model unit cells of $\text{CuIn}_{1.5}\text{Se}_3$ QDs (6 nm diameter by Scherrer analysis). (a) Calculated pattern for a chalcopyrite phase where the calculated intensity of the (211) and (101) reflections exceeds the observed intensity; (b) calculated pattern for an ordered vacancy chalcopyrite phase in agreement with the observed WAXS pattern; and (c) calculated cubic sphalerite phase that lacks the (211) reflection.

of 6 nm $\text{CuIn}_{1.5}\text{Se}_3$ QDs WAXS data began by creating a chalcopyrite model unit cell using experimentally determined copper, indium, and selenium stoichiometries. Copper vacancies (V_{Cu}) were initially placed exclusively on the copper site, resulting in the calculated pattern in Figure 3a. However, the calculated intensities for the (211) and (101) reflections in this model structure exceed the observed WAXS intensities. The indium atoms were then allowed to migrate onto the copper site (In_{Cu}) until the calculated pattern was in agreement with the observed pattern (Figure 3b). A structural model containing In_{Cu} and 2V_{Cu} defect pairs is in agreement with an ordered vacancy chalcopyrite phase. The elemental compositions of all the Cu–In–Se QDs are consistent with the predicted stoichiometries for ordered vacancy Cu–In–Se compounds (Table S2).¹⁷ An alternative cubic sphalerite model unit cell does not adequately describe the observed WAXS pattern (Figure 3c). Attempt at a similar WAXS analysis for smaller Cu–In–Se QDs was complicated by increased broadening of the (211) and neighboring reflections (Figure S4).

The assignment of $\text{CuIn}_{1.5}\text{Se}_3$ and $\text{CuIn}_{2.3}\text{Se}_4$ QDs as chalcopyrite compounds is in agreement with the previously reported chalcopyrite phases of bulk CuInSe_2 and CuIn_3Se_5 .¹⁸ As for CuIn_5Se_8 , only a metastable chalcopyrite phase has been reported in the bulk. Over the crystalline coherence lengths in this work (2–6 nm), chalcopyrite Cu–In–Se QDs were observed over a large range of stoichiometries. In the case of the AgInSe_2 QDs WAXS patterns, it was not possible to distinguish between orthorhombic and hexagonal phases due to the small (3–6 nm) crystalline coherence lengths (Figure S5). AgInSe_2 nanorods have previously been reported in an orthorhombic phase.¹⁹

The observation of PL from Cu–In–Se QDs (QYs up to 25% and decreasing significantly with increasing size) may arise due to the strong confinement of the exciton within the QD. Radiative pathways in the Cu–In–Se QDs appear to remain competitive even in the presence of structural defects, which are known to promote nonradiative relaxation in bulk Cu–In–Se.⁶ In addition, QYs of the AgInSe_2 QDs reached 15%.

The broad PL (~ 100 nm fwhm) observed in the Cu–In–Se QDs arises at least in part from a distribution of QD sizes. It is also possible that a distribution of near band edge trap states, known to arise from shallow donor–acceptor pairs created by defects and vacancies, contributes to the broad PL.¹⁷

In the bulk, CuInSe_2 , CuIn_3Se_5 , and CuIn_5Se_8 have been reported with E_g values of 1.04, 1.21, and 1.15 eV, respectively.¹⁸ The E_g of Cu–In–Se QDs has been tuned here from 1.3 to 1.94 eV (975–640 nm), which is to the blue of the bulk E_g values (Figure S6). We conclude that quantum confinement plays a significant role in determining the E_g of Cu–In–Se QDs,²⁰ while differing elemental compositions may contribute additional small E_g energy variations similar to bulk Cu–In–Se.

The range of E_g values demonstrated by the Cu–In–Se QDs in this work is comparable to the range attainable by thin film copper indium gallium selenide semiconductors (1.0–1.7 eV), which are used in photovoltaic devices.²¹ In addition, the small size and NIR emission of Cu–In–Se QDs make them potentially desirable for biological imaging applications.⁵ The growth of a passivating shell around the Cu–In–Se QDs could enable surface ligand modifications.

In conclusion, we have developed a modular hot injection synthetic method for ternary QDs, composed of commercially available precursors. This synthetic method has the potential to be extended to other QDs composed of I–III–VI semiconductors, allowing for further exploration of the elemental compositions and electronic properties in QD materials.

Acknowledgment. We thank S. Speakman for assistance with WAXS. This work was supported in part by the MIT–Harvard NIH CCNE (1U54-CA119349), the US ARO through the ISN (DAAD-19-02-0002), and the NSF NSEC (DMR-0117795). This work also made use of the shared experimental facilities of the NSF MRSEC program (DMR-0213282) at MIT.

Supporting Information Available: Detailed synthetic procedure, XPS, WAXS, absorbance, PL, and WDS. This material is available free of charge via the Internet at <http://pubs.acs.org>.

References

- (1) Murray, C. B.; Norris, D. J.; Bawendi, M. G. *J. Am. Chem. Soc.* **1993**, *115*, 8706–8715.
- (2) Guzelian, A. A.; Banin, U.; Kadavanich, A. V.; Peng, X.; Alivisatos, A. P. *Appl. Phys. Lett.* **1996**, *69*, 1432–1434.
- (3) Hinds, S.; Myrskog, S.; Levina, L.; Koleilat, G.; Yang, J.; Kelley, S. O.; Sargent, E. H. *J. Am. Chem. Soc.* **2007**, *129*, 7218–7219.
- (4) Huynh, W. U.; Dittmer, J. J.; Alivisatos, A. P. *Science* **2002**, *295*, 2425.
- (5) Zimmer, J. P.; Kim, S. W.; Ohnishi, S.; Tanaka, E.; Frangioni, J. V.; Bawendi, M. G. *J. Am. Chem. Soc.* **2006**, *128*, 2526–2527.
- (6) Shigefusa, C. *Appl. Phys. Lett.* **1997**, *70*, 1840–1842.
- (7) Malik, M. A.; O'Brien, P.; Revaprasadu, N. *Adv. Mater.* **1999**, *11*, 1441.
- (8) Castro, S. L.; Bailey, S. G.; Raffaele, R. P.; Banger, K. K.; Hepp, A. F. *Chem. Mater.* **2003**, *15*, 3142–3147.
- (9) Zhong, H.; Li, Y.; Ye, M.; Zhu, Z.; Zhou, Y.; Yang, C.; Li, Y. *Nanotechnology* **2007**, *18*, 025602.
- (10) Nakamura, H.; Kato, W.; Uehara, M.; Nose, K.; Omata, T.; Otsuka-Yao-Matsuo, S.; Miyazaki, M.; Maeda, H. *Chem. Mater.* **2006**, *18*, 3330.
- (11) Torimoto, T.; Adachi, T.; Okazaki, K. i.; Sakuraoka, M.; Shibayama, T.; Ohtani, B.; Kudo, A.; Kuwabata, S. *J. Am. Chem. Soc.* **2007**, *129*, 12388–12389.
- (12) Steckel, J. S.; Yen, B. K. H.; Oertel, D. C.; Bawendi, M. G. *J. Am. Chem. Soc.* **2006**, *128*, 13032–13033.
- (13) Liu, H.; Owen, J. S.; Alivisatos, A. P. *J. Am. Chem. Soc.* **2007**, *129*, 305.
- (14) Courtney, W. G. *J. Phys. Chem.* **1956**, *60*, 1461–1462.
- (15) Wells, R. L.; Pitt, C. G.; McPhail, A. T.; Purdy, A. P.; Shafieezad, S.; Hallock, R. B. *Chem. Mater.* **1989**, *1*, 4–6.
- (16) Schumann, B.; Tempel, A.; Kühn, G. *Cryst. Res. Technol.* **1988**, *23*, 3.
- (17) Zhang, S. B.; Wei, S.-H.; Zunger, A.; Katayama-Yoshida, H. *Phys. Rev. B* **1998**, *57*, 9642–9656.
- (18) Wasim, S. M.; Rincon, C.; Marin, G.; Delgado, J. M. *Appl. Phys. Lett.* **2000**, *77*, 94–96.
- (19) Ng, M. T.; Boothroyd, C. B.; Vittal, J. J. *J. Am. Chem. Soc.* **2006**, *128*, 7118–7119.
- (20) (a) Brus, L. E. *J. Chem. Phys.* **1984**, *80*, 4403–4409. (b) The effective mass approximation overstates the degree of quantum confinement for the small QDs (radii 1.0–1.5 nm) presented in this work.
- (21) Ramanathan, K.; Teeter, G.; Keane, J. C.; Noufi, R. *Thin Solid Films* **2005**, *480–481*, 499–502.

JA8036349